



HAL
open science

Identification of the Ricin Lipase Site and Implication in Cytotoxicity

Juliette Morlon-Guyot, Mohamed Helmy, Sophie Lombard-Frasca, David Pignol, Gérard Pieroni, Bruno Beaumelle

► **To cite this version:**

Juliette Morlon-Guyot, Mohamed Helmy, Sophie Lombard-Frasca, David Pignol, Gérard Pieroni, et al.. Identification of the Ricin Lipase Site and Implication in Cytotoxicity. *Journal of Biological Chemistry*, 2003, 278 (19), pp.17006-17011. 10.1074/jbc.M209516200 . hal-02998151

HAL Id: hal-02998151

<https://hal.science/hal-02998151>

Submitted on 10 Nov 2020

HAL is a multi-disciplinary open access archive for the deposit and dissemination of scientific research documents, whether they are published or not. The documents may come from teaching and research institutions in France or abroad, or from public or private research centers.

L'archive ouverte pluridisciplinaire **HAL**, est destinée au dépôt et à la diffusion de documents scientifiques de niveau recherche, publiés ou non, émanant des établissements d'enseignement et de recherche français ou étrangers, des laboratoires publics ou privés.

Identification of the Ricin Lipase Site and Implication in Cytotoxicity*

Received for publication, September 17, 2002, and in revised form, February 26, 2003
Published, JBC Papers in Press, February 28, 2003, DOI 10.1074/jbc.M209516200

Juliette Morlon-Guyot‡, Mohamed Helmy§¶, Sophie Lombard-Frasca§, David Pignoll||, Gérard Piéroni§**, and Bruno Beaumelle‡ ††

From the ‡UMR 5539 CNRS, Département Biologie-Santé, Université Montpellier II, 34095 Montpellier, §U 476 INSERM, Faculté de Médecine, 27 Boulevard Jean Moulin, 13385 Marseille, and ||Laboratoire de Bioénergétique Cellulaire, Département d'Ecophysiologie Végétale et Microbiologie, CEA-Cadarache, 13107 Saint Paul lez Durance, France

Ricin is a heterodimeric plant toxin and the prototype of type II ribosome-inactivating proteins. Its B-chain is a lectin that enables cell binding. After endocytosis, the A-chain translocates through the membrane of intracellular compartments to reach the cytosol where its N-glycosidase activity inactivates ribosomes, thereby arresting protein synthesis. We here show that ricin possesses a functional lipase active site at the interface between the two subunits. It involves residues from both chains. Mutation to alanine of catalytic serine 221 on the A-chain abolished ricin lipase activity. Moreover, this mutation slowed down the A-chain translocation rate and inhibited toxicity by 35%. Lipase activity is therefore required for efficient ricin A-chain translocation and cytotoxicity. This conclusion was further supported by structural examination of type II ribosome-inactivating proteins that showed that this lipase site is present in toxic (ricin and abrin) but is altered in nontoxic (ebu- lin 1 and mistletoe lectin I) members of this family.

Ricin, isolated from seeds of the plant *Ricinus communis*, is the prototype of type II ribosome-inactivating proteins (RIPs)¹ and one of the most powerful toxins capable of killing animal cells. This 66-kDa glycoprotein is composed of two chains (RTA and RTB) linked *via* a disulfide bond. RTA is responsible for cytotoxicity. This N-glycosidase catalyzes the depurination of a specific adenine on the 28 S ribosomal RNA, thereby inactivating protein synthesis and leading to cell death. RTB is a lectin that recognizes terminal galactose residues and is responsible for toxin binding to cells (1).

X-ray structures of the heterodimer and the recombinant RTA subunit (rRTA) have been solved at 2.5 and 2.3 Å, respectively (2, 3). These studies described both the RTA N-glycosidase active site and the RTB galactose binding pockets. rRTA lacks the glycans present on native RTA but shows complete biological activity (1, 4).

Ricin has been used to study molecular mechanisms involved in intracellular trafficking (5). After cell binding, ricin is endo-

cytosed and can be visualized in endosomes and the *trans*-Golgi network (6). Biochemical evidence indicates that it could be transported back to the endoplasmic reticulum (7). Ricin escape to the cytosol has been reported to occur from endosomes (8), the Golgi apparatus (9), and the endoplasmic reticulum (7). It is not known whether the affinity of RTA for model membranes (10, 11) facilitates its *trans*-membrane transport. This translocation step is rate-limiting for cytotoxicity (12).

Ricin has been extensively studied for its potential use in cancer treatments. Toward this objective, immunotoxins (ITs) were prepared by attaching ricin to a monoclonal antibody (13). For clinical use and to avoid nonspecific binding of the IT, B-chain lectin sites were chemically inactivated. ITs containing such blocked ricin are usually much more efficient *in vivo* than those prepared with RTA alone (13). Similar data were obtained *in vitro* when lactose was used to prevent RTB binding to cells, *i.e.*, ricin-containing ITs were more toxic than ITs made from RTA (14). Hence, RTB involvement in ricin toxicity is not restricted to cell binding mediated by its lectin sites (15). The basis of this potentiation effect of RTB on RTA toxicity, even when RTB lectin activity is ineffective, is not known.

Following our initial observation that ricin displays significant homology to a lipase from another Euphorbiaceae (16), we recently demonstrated that ricin shows lipolytic activity (17) and further characterized its specificity toward neutral lipids (18). Such lipase activity could facilitate RTA access to the cytosol by providing local destabilization of the membrane (18) and might therefore be implicated in the potentiation of RTA toxicity by RTB. The B-chain would thus directly assist the A-chain during its translocation step as is the case for another heterodimeric toxin, diphtheria toxin (19).

In this study, we localized a single canonical lipase catalytic triad within ricin and localized at the junction between RTA and RTB. We demonstrated the functionality of the ricin lipase site, which is conserved in toxic but not in innocuous members of the type II RIP family.

EXPERIMENTAL PROCEDURES

Materials—Ricin, CM- and Blue-Sepharose, and most chemicals were obtained from Sigma. [³⁵S]methionine (Trans-label) was from ICN. Pure RTB (without any detectable RTA) was purchased from Inland Labs (Austin, TX). RTA was purified from a commercial preparation (Sigma) using chromatography on lactose-agarose (8) to remove contaminating ricin. Transferrin was labeled with Cy5 using a labeling kit (Amersham Biosciences). Secondary antibodies for immunofluorescence were from Nordick.

Mutagenesis—The full-length RTA coding sequence (20) in pKK 223.3 (Pharmacia) was used as a template for PCR-based mutagenesis (21). A 5'-mutagenic primer GCAATTCAAGAGGCTAACCAAGGAGCC, in which the TCT coding for Ser-221 was changed to the underlined GCT (Ala), was used together with a 3'-primer overlapping the downstream plasmid-*Hind*III site to prepare a first PCR fragment. A 3'-

* The costs of publication of this article were defrayed in part by the payment of page charges. This article must therefore be hereby marked "advertisement" in accordance with 18 U.S.C. Section 1734 solely to indicate this fact.

¶ Recipient of a grant from the French government.

** Supported by the Conseil Général des Bouches du Rhône.

†† To whom correspondence should be addressed: UMR 5539 CNRS, Case 107, Université Montpellier II, 34095 Montpellier Cedex 05, France. Tel.: 33-467-14-33-98; Fax: 33-467-14-42-86; E-mail: beaumel@univ-montp2.fr.

¹ The abbreviations used are: RIP, ribosome-inactivating protein; RTA, ricin toxin A-chain; RTB, RT B-chain; rRTA, recombinant RTA; ITs, immunotoxins; TRITC, tetramethylrhodamine isothiocyanate.

mutagenic primer and a 5'-primer spanning the upstream *ClaI* site enabled obtaining a second PCR fragment. These overlapping fragments were then joined and amplified by a second PCR using the outer primers. The resulting *ClaI-HindIII* fragment was inserted into pKK 223.3-RTA for expression. A similar strategy was adopted to change His-40 to Ala, using a 5'-mutagenic primer in which the CAT coding for His-40 was altered to GCT (Ala), together with a 3'-primer covering the *ClaI* site. The upstream fragment was prepared using a 5'-primer covering the plasmid *EcoRI* site and a 3'-mutagenic primer prior to the second round of PCR run to join the fragments. PCR-amplified DNA was entirely sequenced.

Purification and RNA N-Glycosidase Assays of rRTA and rRTA Mutants—A 1.5-liter culture of transfected *Escherichia coli* TG2 was grown at 30 °C. Expression was induced at an A_{595} of ~0.7, using 1 mM isopropylthiogalactoside. After 2.5 h at 30 °C, *E. coli* lysates were prepared by sonication, clarified by centrifugation for 30 min at 25,000 × *g*, and dialyzed against 10 mM sodium phosphate buffer, pH 6.8 (buffer A), before loading onto a CM-Sepharose column. After washing with buffer A, rRTA was eluted with a NaCl gradient of 0–1 M in buffer A (20). A-chains were further purified by affinity chromatography on Blue-Sepharose and assayed for N-glycosidase activity using rabbit reticulocyte lysates (Promega) as indicated (8).

Association of rRTA with RTB—Equimolar amounts of rRTA and plant RTB (20 μM in phosphate-buffered saline) were mixed in the presence of 8 mM reduced glutathione. After 3 h at room temperature and overnight dialysis at 4 °C against phosphate-buffered saline (4), the reconstituted control or mutated ricins were filtered-sterilized and stored at 4 °C for up to 1 week.

Lipase and Toxicity Assays—RTA, rRTA, RTB, native, control, or mutant ricins (0–150 nmol) were added to 1 ml of 100 mM Tris-HCl, pH 8.0, containing 2 mM 5,5'-dithiobis(2-nitrobenzoic acid) and 2 mM of 2,3-dimercapto-1-propanol tributyrates (BAL-TC₄; Aldrich). After 30 min at 37 °C, 2 ml of acetone were added before measuring the A_{412} as described previously (18). Specific lipolytic activities were expressed as millikatal/mol. A katal is the amount of enzyme which transforms 1 mol of substrate per second. Bovine serum albumin, used as control, did not show any lipolytic activity. Peripheral blood mononuclear cells were purified from human blood using Ficoll-Paque plus (Amersham Biosciences), and monocytes were allowed to adhere overnight to tissue culture plates before washing and adding ricins. After 24 h, the medium (RPMI complemented with 10% human AB⁺ serum) was replaced for 4 h with Dulbecco's modified Eagle's medium without methionine, supplemented with [³⁵S]methionine. This medium was then aspirated. Cell proteins were precipitated with trichloroacetic acid and collected by filtration before scintillation counting (4). Experiments were performed in triplicate and repeated three times. Errors are expressed as S.E.

Kinetics of Protein Synthesis Inactivation by Control or Mutated Ricin—A431 cells in Dulbecco's modified Eagle's medium containing 10% fetal calf serum were seeded into 96-well plates (24,000 cells/well), whereas monocytes were used at 40–60,000 cells/well. Ricins were added, and a 1-h (A431) or 2-h (monocytes) pulse incorporation of [³⁵S]methionine in Dulbecco's modified Eagle's medium without methionine was performed at various times after the start of intoxication (4).

Internalization Studies—Ricins were radiolabeled with ¹²⁵I to monitor their endocytosis efficiency at 37 °C by mouse BW 5147 lymphocytes, using 0.1 M lactose to displace plasma membrane-bound ricin molecules (4). For fluorescence microscopy, A431 cells were labeled for 40 min at 37 °C with 30 nM ricin and 200 nM transferrin-Cy5 in Dulbecco's modified Eagle's medium supplemented with 0.2 mg/ml bovine serum albumin before lactose scraping. Cells were further washed, fixed, permeabilized with 0.015% saponin, and labeled with antibodies. The rabbit anti-ricin antibodies (Sigma) were revealed using TRITC-labeled swine anti-rabbit IgG; sheep anti-TGN46 (Serotec) and the H4A3 anti-Lamp-1 monoclonal antibody (Iowa Developmental Studies Hybridoma Bank) were detected using fluorescein isothiocyanate-conjugated donkey anti-sheep and goat anti-mouse antibodies, respectively. After mounting, cells were examined under a Leica confocal microscope (22).

Structure Analysis—Structures of ricin (PDB code 2AAI), neutral *Pseudomonas* lipase (5TGL), abrin (1ABR) mistletoe lectin I (1CE7), and ebulin (1HWO) were analyzed using the graphic program O (23) running on a Silicon Graphics workstation.

RESULTS AND DISCUSSION

We first tried to identify the ricin chain responsible for heterodimer lipase activity. Purified chains showed lipase activities below 18% as compared with native ricin (Fig. 1A). We

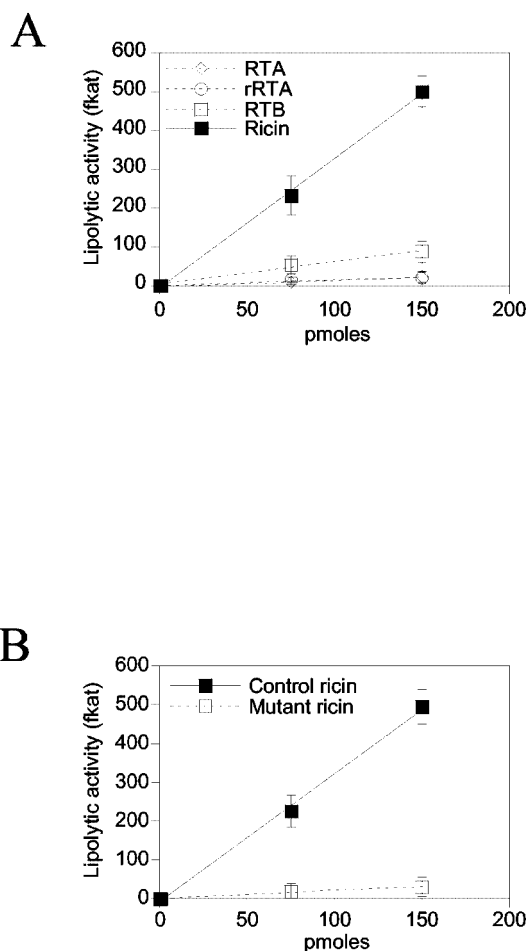


FIG. 1. Lipolytic activity of ricin chains, native, control, and mutated (rRTA221A) ricin. Proteins were assayed for lipase activity at 37 °C using BAL-TC₄ as substrate. Activities are expressed as femtokatal. A, native ricin, RTA, rRTA, and RTB. B, control (rRTA-RTB) and mutant (rRTA221A-RTB) ricin.

concluded that the lipase site is found in the heterodimer only.

Localization of a Putative Catalytic Triad—All lipolytic enzymes investigated so far vary widely in size and amino acid sequence. However, most of them belong to the α/β hydrolase superfamily in which the catalytic machinery consists of a nucleophile, an acid, and a histidine residue (the catalytic triad). Nucleophilic serine is located at the center of an extremely sharp turn between a β -strand and an α -helix. The sharpness of the turn results in phi and psi angles that lie in an unfavorable region of the Ramachandran plot (24). A specific feature of lipases, as compared with canonical α/β hydrolases, is that the active site is inaccessible to substrate in solution. In the presence of lipids, unmasking the active site generates the hydrophobic substrate binding site. This conformational change generates the so-called oxyanion hole where the transition state of the reaction can be stabilized via hydrogen bonds with two main-chain nitrogens (25).

Ricin lipase activity is more active (~5-fold) on neutral lipids, such as triglycerides (18), than on glycerophospholipids (17). We therefore investigated the crystal structure of ricin to find common structural features with α/β hydrolases, using the typical neutral lipase of *Pseudomonas* as reference (26). This led us to find only one putative serine hydrolase catalytic triad (RTA-Ser-221, RTA-His-40, and RTB-Asp-94). Nucleophilic RTA-Ser-221 is located at the beginning of a small turn between an α -helix (from 202 to 220) and a β -strand (from 227 to 234) (Fig. 2). Nevertheless, as opposed to α/β hydrolases, the

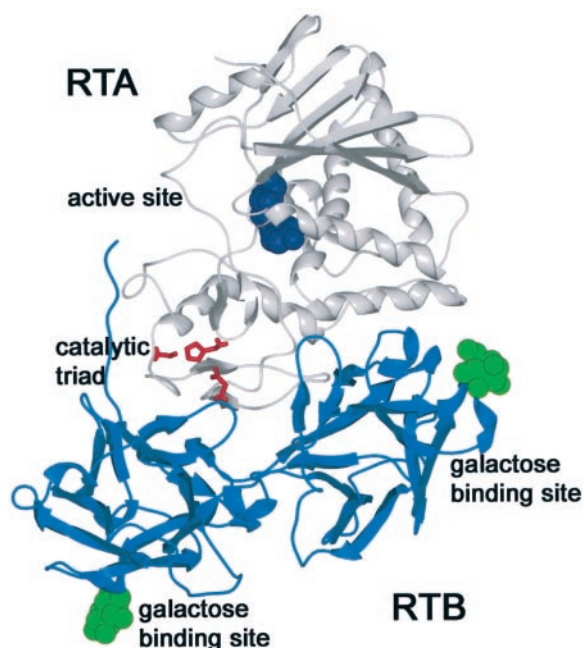


FIG. 2. **Ribbon structure of ricin with its different active sites.** The figure was drawn with SPOCK (quorum.tamu.edu/jon/spock/). RTA is light gray and RTB is blue. At the interface of both subunits, side chains of the lipase catalytic triad are shown as red sticks. Key residues of the RTA depurination active site and of RTB galactose binding sites are shown as blue and green Corey-Pauling-Koltun (CPK), respectively.

catalytic serine lies in a favorable region of the Ramachandran plot. RTA-Ser-221 is hydrogen-bonded to RTA-His-40, which in turn interacts with Asp-94 of the RTB subunit. The distances between RTA-Ser-221 $\text{o}\gamma$ and RTA-His-40 $\text{N}\epsilon 2$ and between RTA-His-40 $\text{N}\delta 1$ and RTB-Asp-94 $\text{o}\delta$ are 3.2 and 2.8 Å, respectively. These values are almost identical to those measured in our reference lipase active site (3.1 and 2.8 Å). Hence, the relative orientation of side chains involved in both catalytic triads are strikingly similar, whereas ricin and lipase folding is completely different (Fig. 3, A and B). RTA-Ser-221 is located at the bottom of a hydrophobic groove, which might correspond to the binding site of substrate acyl chains. No attempt was made here to model a putative conformational change similar to lipase activation. The putative substrate binding site is located at the interface between ricin subunits (Fig. 3B). Such localization explains why the heterodimer only shows significant lipase activity (Fig. 1A).

The Putative Lipase Catalytic Site Is Functional—Among the three residues of the putative catalytic triad, two of them, RTA-His-40 and RTB-Asp-94, directly interact and are involved in A/B polar interactions (27). Accordingly, when rRTA-His-40 was changed to Ala and produced in *E. coli*, the resulting rRTA40A associated very poorly with RTB as compared with control rRTA (Fig. 4). Not surprisingly, this rRTA40A-RTB preparation, containing a large proportion (~80%) of isolated chains, did not show significant lipase activity (data not shown). Because this mutation prevented heterodimer formation, and therefore building of the lipase site, it was not possible to deduce from this lack of lipase activity any information regarding the role of RTA-His-40 in lipase activity. RTA-His-40 and RTB-Asp-94 only interact with each other across the A/B interface (27). An RTB-Asp-94 mutation would thus likely destabilize the heterodimer exactly as the rRTA-H40A change, and so we did not prepare such a mutant.

The third residue of the ricin lipase site, RTA-Ser-221, is not implicated in A/B interaction and was potentially catalytic. It was therefore the most appropriate for a point mutation in

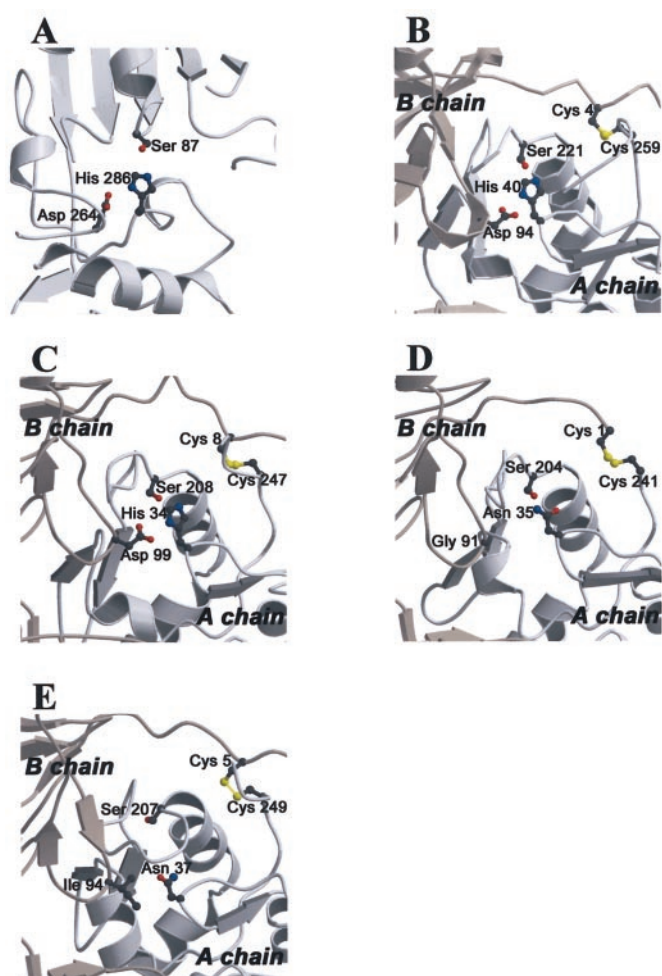


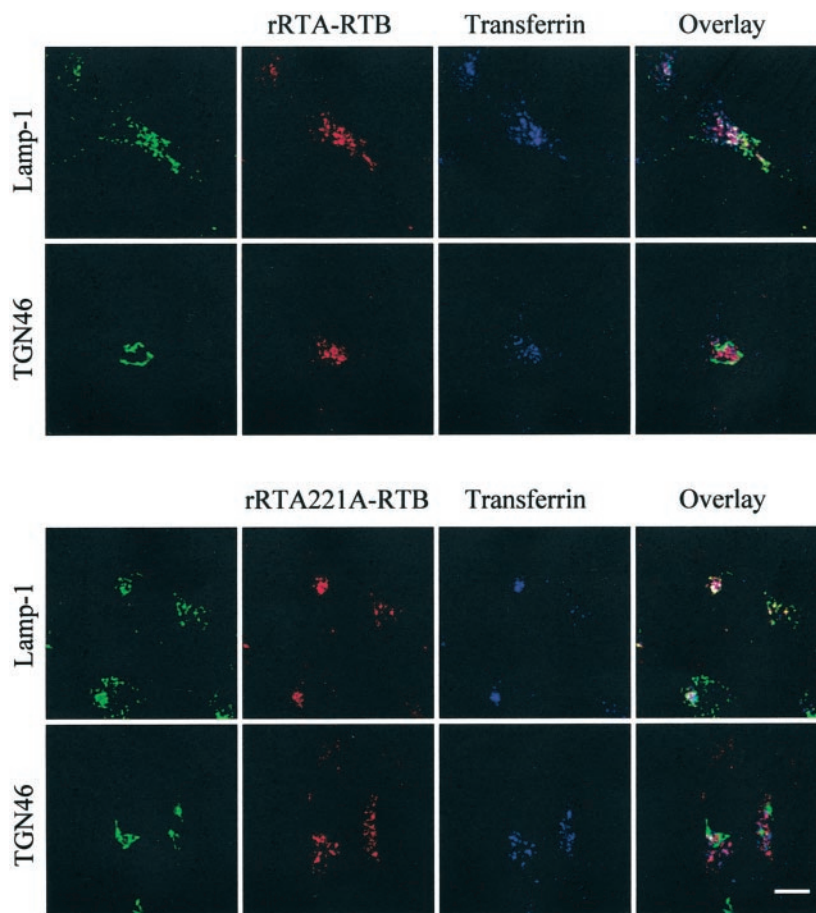
FIG. 3. **Localization of the catalytic triad in *Pseudomonas* neutral lipase and type II RIPS.** A, *Pseudomonas* neutral lipase. B, ricin. C, abrin. D, mistletoe lectin I. E, ebulin I. Toxin subunits, depicted in gray (B-chain) or brown (A-chain), are disulfide-linked via the highlighted cysteine residues. The catalytic triad (shown as sticks) is present in ricin and abrin but not conserved in the two latter RIPS, which are not (39) or weakly (38) toxic. Structures were represented using Molscript (40).



FIG. 4. **Association of control and mutant rRTA with RTB.** Equimolecular amounts of B-chain and the indicated A-chain were treated with reduced glutathione. After dialysis, an aliquot of the mixture was separated using non-reducing SDS-PAGE. Gels were Coomassie Blue stained. The positions of the heterodimer (A-B) and isolated monomers (A and B) are shown.

order to study the functionality of this site. We replaced rRTA-Ser-221 by an alanine. The rRTA221A mutant was produced in *E. coli*. It could form the heterodimer as efficiently as control rRTA (Fig. 4). Again, this was not surprising because Ser-221 does not interact with any B-chain residue (27). RTA-Ser-221 is located far away from the N-glycosidase active site cleft (around 25 Å). Nevertheless, several amino acids outside this

FIG. 5. Ricin intracellular routing is not affected by the RTA221A mutation. A431 cells were incubated for 40 min at 37 °C with transferrin-Cy5 and either control (rRTA-RTB) or mutant (rRTA221A-RTB) ricin. After removing plasma membrane-bound ricin using 0.1 M lactose, cells were fixed and processed for immunofluorescence staining of ricin, TGN46, or Lamp-1 as indicated. Representative medial optical section obtained using a confocal microscope. Bar, 10 μ m.



cleft can, albeit indirectly, participate in *N*-glycosidase catalysis (28). Hence, it was important to check whether the S221A mutation affected this activity. We therefore tested the abilities of RTA, rRTA, rRTA40A, and rRTA221A to inhibit cell-free protein synthesis in reticulocyte lysates. No significant difference in *N*-glycosidase activity was found (not shown). We therefore concluded that the rRTA221A mutation did not affect the ribosome-inactivating activity of the protein.

We then compared the properties of these control (rRTA-RTB) and mutant (rRTA221A-RTB) ricins. Wild-type (RTA-RTB) and control (rRTA-RTB) ricins displayed indistinguishable lipase activities: ~ 3.3 millikatal/mol (Fig. 1, A and B) on BAL-TC₄. This demonstrates that the lipase active site of ricin is correctly assembled upon formation of control ricin. The S221A mutation on the A-chain decreased heterodimer lipase activity to non-significant levels, corresponding to a $94 \pm 5\%$ inhibition compared with control ricin (Fig. 1B). This demonstrates the catalytic role of RTA-Ser-221 in lipid hydrolysis and is consistent with the 89% inhibition obtained using a serine hydrolase inhibitor, *i.e.* E₆₀₀ (18). The lipase site predicted by structural analysis is therefore functional in ricin and unique within the molecule.

Lipase Activity Does Not Affect Ricin Intracellular Routing—We then assessed the involvement of ricin lipolytic activity in its intracellular transport using rRTA221-RTB. Cell binding and global endocytosis efficiency were monitored *via* the uptake of ¹²⁵I-ricin by mouse lymphocytes (4). This assay did not reveal any difference between control and mutant ricin (not shown). Ricin intracellular routing was examined by immunofluorescence confocal microscopy using fluorescent transferrin, TGN46, and Lamp-1 as markers of early endosomes (22), the *trans*-Golgi network (29), late endosomes and lysosomes (30), respectively. Both control and mutant ricins were

efficiently endocytosed by A431 cells (Fig. 5). Consistent with numerous studies of ricin uptake by several cell types (8, 31, 32), they localized essentially to elements of the endo/lysosomal pathway, together with transferrin and Lamp-1. In agreement with previous data demonstrating the transport of a small fraction of endocytosed ricin to the *trans*-Golgi network (31), weak colocalization of ricins with TGN46 was observed. Control and mutant ricins (shown in Fig. 5 for control and S221A, not shown for H40A) displayed the same intracellular pathway when studied through this assay. We concluded that lipolytic activity is not involved in ricin intracellular trafficking.

Lipase Activity Is Implicated in Ricin Cytotoxicity and Translocation—We then tested whether mutations within a ricin lipase site would affect toxicity, using monocytes from human peripheral blood as target cells. rRTA221A-RTB with an IC₅₀ of 3 pM was $\sim 35\%$ less toxic than control ricin (rRTA-RTB), which showed an IC₅₀ of 2 pM for these cells (Fig. 6). rRTA40A-RTB was the least toxic molecule (IC₅₀ of 10 pM), probably because of the weak A/B interaction for this mutant.

Ricin translocation was examined using kinetics of protein synthesis inactivation. This assay enables translocation assessment on intact cells (4, 12). It therefore provides data that are not restricted to the observation of ricin translocation from a specific organelle. The slope of the plot log (protein synthesis) *versus* time, measured after the initial dose-dependent lag, is directly proportional to the RTA translocation rate (12). As shown in Fig. 7A for A431 cells and Fig. 7B for monocytes, mutant ricin (rRTA221A-RTB) killed cells more slowly than the control toxin. Because the mutation did not affect rRTA *N*-glycosidase activity or intracellular routing, the difference in the cell-killing rate was because of a lower translocation efficiency of mutant rRTA. When translocation rates were calculated from the best slope of these plots, whatever the cell line,

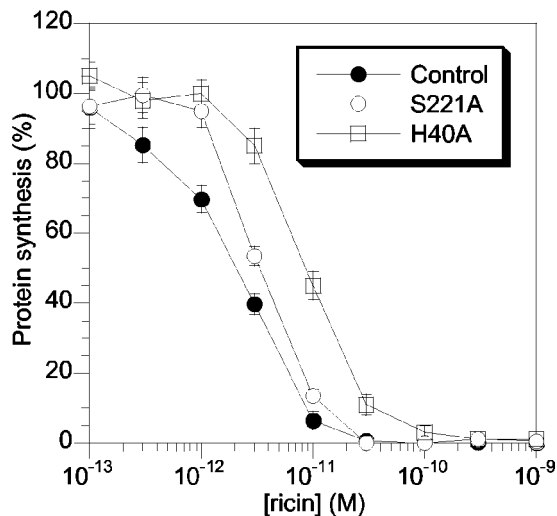


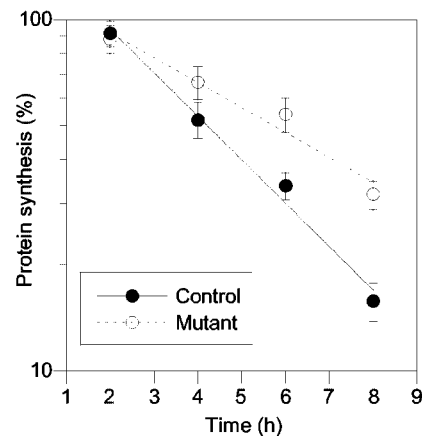
FIG. 6. **Inactivation of ricin lipase activity inhibits cytotoxicity.** Human monocytes were treated with the indicated ricin for 24 h before assaying protein synthesis using [³⁵S]methionine. Results from a typical experiment that was repeated three times using blood from different donors.

rRTA221A translocation efficiency was only $64 \pm 5\%$ (mean \pm S.E.; $n = 7$; $p < 0.001$) compared with that of rRTA. This result demonstrates that ricin lipase activity is implicated in toxicity, presumably during the translocation step. Although the effect of the RTA221A mutation on cytotoxicity and translocation may appear moderate, it should be noted that conjugates made only from RTA are already toxic, showing that, once bound to cells, RTA is able to translocate quite efficiently on its own. Nevertheless, conjugates prepared using blocked ricin are usually more efficient (13). Second, ricin lipase activity is low (18). We therefore propose that the lipase activity of the heterodimer is likely responsible for this potentiation effect of the B-chain even when lectin sites are inactivated (14). The B-chain therefore assists and facilitates A-chain translocation within the animal cell. Interestingly, compartments where ricin translocation was reported to take place, such as late endosomes (4) and the endoplasmic reticulum (7), are specifically enriched in triglycerides compared with the plasma membrane (33, 34). Because these lipid species are the preferred substrate for ricin lipase activity (18), potentiation of A-chain translocation likely results from local destabilization of the membrane of specific, triglycerides-rich intracellular compartments by moderate lipase activity of the heterodimer.

Mutation of RTA-His-40 did not give rise to a mutant suitable for studying the role of this residue in lipase activity, because the mutation prevented the A/B association required to generate the site. Hence, suppression of a single point of A/B interaction among the 15 pairs of residues enabling stabilization of the heterodimer (in addition to the interchain disulfide) (27) led to a dramatic heterodimer dissociation. Because the heterodimer does not show any RNA *N*-glycosidase activity, the A-chain has to be released at a late stage of the intoxication process, presumably following reduction of the interchain disulfide (35). The A/B interaction, which showed a K_d in the micromolar range (36), is therefore easily reversible; it was not very surprising that removing one point of interaction *via* the RTA40A mutation induced massive dissociation.

The ricin lipase site is, to our knowledge, the first ever reported to be constituted by residues from distinct subunits. This could be a feature of plant lipases, and ricin is the first one whose structure is available. Because ricin is the prototype of type II RIPs, it was interesting to examine whether the lipase

A



B

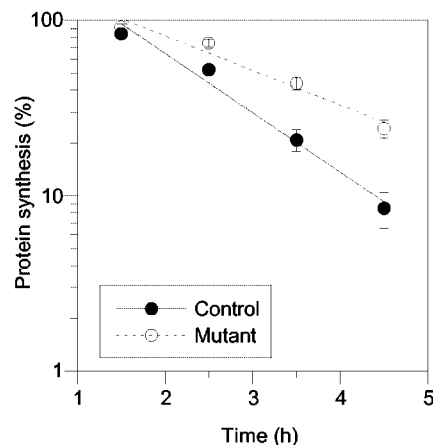


FIG. 7. **Kinetics of cell protein synthesis inactivation by control or mutated ricin.** A431 cells (A) or monocytes (B) were incubated for various times with 400 pM (A) or 100 pM (B) control (rRTA-RTB) or mutant (rRTA221A-RTB) ricin and then pulsed with [³⁵S]methionine to measure protein synthesis. Plots of log protein synthesis *versus* the incubation time plus one-half the [³⁵S]methionine pulse time. Linear regression curves are shown ($0.95 < r < 1$), and their slopes were used to compare the efficiency of A-chain translocation. Plots are from typical experiments that were repeated three times.

site was also present in other members of this family whose structures are available. Abrin, a toxin structurally and functionally related to ricin (37), also displays a potential lipase catalytic site made of Ser-208 (A-chain), His-34 (A-chain), and Asp-99 (B-chain) (Fig. 3C). Structural analysis clearly showed (Fig. 3) that the lipolytic site is not conserved in the two barely toxic type II RIPs, mistletoe lectin I (38) and ebulin 1 (39). Hence, there is a correlation between the presence of a canonical lipase site and toxicity in type II RIPs. This finding further indicates that lipolytic activity likely plays an important role in their cytotoxicity.

REFERENCES

- Lord, J. M., Roberts, L. M., and Robertus, J. D. (1994) *FASEB J.* **8**, 201–208
- Montfort, W., Villafranca, J. E., Monzingo, A. F., Ernst, S. R., Katzin, B., Rutember, E., Xuong, N. H., Hamlin, R., and Robertus, J. D. (1987) *J. Biol. Chem.* **262**, 5398–5403
- Mlsna, D., Monzingo, A. F., Katzin, B. J., Ernst, S., and Robertus, J. D. (1993) *Protein Sci.* **2**, 429–435

4. Beaumelle, B., Taupiac, M. P., Lord, J. M., and Roberts, L. M. (1997) *J. Biol. Chem.* **272**, 22097–22102
5. Sandvig, K., and van Deurs, B. (2000) *EMBO J.* **19**, 5943–5950
6. van Deurs, B., Tonnessen, T. I., Petersen, O. W., Sandvig, K., and Olsnes, S. (1986) *J. Cell Biol.* **102**, 37–47
7. Wesche, J., Rapak, A., and Olsnes, S. (1999) *J. Biol. Chem.* **274**, 34443–34449
8. Beaumelle, B., Alami, M., and Hopkins, C. R. (1993) *J. Biol. Chem.* **268**, 23661–23669
9. Bilge, A., Warner, C. V., and Press, O. W. (1995) *J. Biol. Chem.* **270**, 23720–23725
10. Utsumi, T., Ide, A., and Funatsu, G. (1989) *FEBS Lett.* **242**, 255–258
11. Day, P. J., Pinheiro, T. J., Roberts, L. M., and Lord, J. M. (2002) *Biochemistry* **41**, 2836–2843
12. Hudson, T. H., and Neville, D. M. (1987) *J. Biol. Chem.* **262**, 16484–16494
13. Kreitman, R. J. (1999) *Curr. Opin. Immunol.* **11**, 570–578
14. Gregg, E. O., Bridges, S. H., Youle, R. J., Longo, D. L., Houston, L. L., Glennie, M. J., Stevenson, F. K., and Green, I. (1987) *J. Immunol.* **138**, 4502–4508
15. Frankel, A. E., Fu, T., Burbage, C., Chandler, J., Willingham, M. C., and Tagge, E. P. (1997) *Leukemia* **11**, 22–30
16. Moulin, A., Teissere, M., Bernard, C., and Pieroni, G. (1994) *Proc. Natl. Acad. Sci. U. S. A.* **91**, 11328–11332
17. Helmy, M., Lombard, S., and Piéroni, G. (1999) *Biochem. Biophys. Res. Commun.* **258**, 252–255
18. Lombard, S., Helmy, M. E., and Pieroni, G. (2001) *Biochem. J.* **358**, 773–781
19. Falnes, P. O., and Sandvig, K. (2000) *Curr. Opin. Cell Biol.* **12**, 407–413
20. Chaddock, J. A., and Roberts, L. M. (1993) *Protein Eng.* **6**, 425–431
21. Landt, O., Grunert, H.-P., and Hahn, U. (1990) *Gene* **96**, 125–128
22. Alami, M., Taupiac, M. P., Reggio, H., Bienvenue, A., and Beaumelle, B. (1998) *Mol. Biol. Cell* **9**, 387–402
23. Jones, T. A., Zou, J. Y., Cowan, S. W., and Kjeldgaard, M. (1991) *Acta Crystallogr. Sect. A* **47**, 110–119
24. Ollis, D. L., Cheah, E., Cygler, M., Dijkstra, B., Frolow, F., Franken, S. M., Harel, M., Remington, S. J., Silman, I., and Schrag, J. (1992) *Protein Eng.* **5**, 197–211
25. Jaeger, K. E., Ransac, S., Dijkstra, B. W., Colson, C., van Heuvel, M., and Misset, O. (1994) *FEMS Microbiol. Rev.* **15**, 29–63
26. Schrag, J. D., Li, Y., Cygler, M., Lang, D., Burgdorf, T., Hecht, H. J., Schmid, R., Schomburg, D., Rydel, T. J., Oliver, J. D., Strickland, L. C., Dunaway, C. M., Larson, S. B., Day, J., and McPherson, A. (1997) *Structure* **5**, 187–202
27. Rutenber, E., and Robertus, J. D. (1991) *Proteins* **10**, 260–269
28. Kitaoka, Y. (1998) *Eur. J. Biochem.* **257**, 255–262
29. Rohrer, J., and Kornfeld, R. (2001) *Mol. Biol. Cell* **12**, 1623–1631
30. Gruenberg, J., and Maxfield, F. R. (1995) *Curr. Opin. Cell Biol.* **7**, 552–563
31. van Deurs, B., Sandvig, K., Peterson, O. W., Olsnes, S., Simons, K., and Griffiths, G. (1988) *J. Cell Biol.* **106**, 253–267
32. van Deurs, B., Hansen, S. H., Petersen, O. W., Melby, E. L., and Sandvig, K. (1990) *Eur. J. Cell Biol.* **51**, 96–109
33. Kobayashi, T., Stang, E., Fang, K. S., de Moerloose, P., Parton, R. G., and Gruenberg, J. (1998) *Nature* **392**, 193–197
34. Hussain, M. M. (2000) *Atherosclerosis* **148**, 1–15
35. Olsnes, S., Sandvig, K., Refsnes, K., and Pihl, A. (1976) *J. Biol. Chem.* **251**, 3985–3992
36. Lewis, M. S., and Youle, R. J. (1986) *J. Biol. Chem.* **261**, 11571–11577
37. Tahirov, T. H., Lu, T. H., Liaw, Y. C., Chen, Y. L., and Lin, J. Y. (1995) *J. Mol. Biol.* **250**, 354–367
38. Eschenburg, S., Krauspenhaar, R., Mikhailov, A., Stoeva, S., Betzel, C., and Voelter, W. (1998) *Biochem. Biophys. Res. Commun.* **247**, 367–372
39. Pascal, J., Day, P. J., Monzingo, A. F., Ernst, S. R., Robertus, J. D., Iglesias, R., Perez, Y., Ferreras, J. M., Citores, L., and Girbes, T. (2001) *Proteins* **43**, 319–326
40. Kraulis, P. J. (1991) *J. Appl. Crystallogr.* **24**, 946–950